photonics

MDPI

Article

Motion of Dissipative Solitons in Quasi-One-Dimensional Potentials

Valentin Besse [1], Hervé Leblond [1,*], Dumitru Mihalache [2] and Boris A. Malomed [3,4]

[1] Laboratoire de Photonique d'Angers, EA 4464, Université d'Angers, LUNAM Université, 2 Boulevard Lavoisier, 49000 Angers, France; valentinbesse@aumbox.net
[2] Horia Hulubei National Institute of Physics and Nuclear Engineering, Magurele, 077125 Bucharest, Romania; dumitru.mihalache@nipne.ro
[3] Department of Physical Electronics, School of Electrical Engineering, Faculty of Engineering, Tel Aviv University, Tel Aviv 69978, Israel; malomed@tauex.tau.ac.il
[4] Instituto de Alta Investigación, Universidad de Tarapacá, Casilla 7D, Arica 1001236, Chile
* Correspondence: herve.leblond@univ-angers.fr

Abstract

We consider the motion of two-dimensional (2D) dissipative solitons and soliton pairs in the framework of the cubic–quintic complex Ginzburg–Landau equation with quasi-1D, spatially periodic or radial lattice potentials. The equation is solved numerically for inputs representing one or two fundamental solitons, which are set in motion by a kick. For the quasi-1D potential, the kick parallel to the potential axis naturally initiates the free motion of the 2D solitons, as the model remains Galilean-invariant in this direction. Motion in the transverse direction, which may entail pulse multiplication, commences if the kick is strong enough. Oblique kicks lead to the straightforward superposition of the longitudinal and transverse motions. Also considered is the collision between 2D solitons moving in the longitudinal and diagonal directions. In the radial potential, the soliton kicked towards the center may bounce back from the central potential hill or pass it, producing complex trajectories and the splitting of the moving soliton.

Keywords: complex Ginzburg–Landau equation; dissipative soliton; quasi-1D potential

1. Introduction

The complex Ginzburg–Landau (CGL) equation has been the subject of extensive research over the course of several decades; see Ref. [1] for a review of earlier works. A well-known species of modes generated by one-dimensional (1D) CGL equations is self-trapped localized states in the form of dissipative solitons [2–7]. They are supported by coexisting balances between dispersion or diffraction and nonlinearity, as in the case of conservative solitons, and between gains and losses.

Multidimensional solitons, including optical spatiotemporal ones in the form of "light bullets" [8,9], have also drawn a great deal of interest. A crucially important issue for multidimensional solitons is their instability against critical or supercritical collapse [10]. In particular, the stabilization of 2D and 3D solitons, including those with embedded vorticity, can be readily provided by competing nonlinearities, which is often represented by the combination of cubic self-focusing and quintic defocusing terms [11–17]. The cubic–quintic nonlinearity can also secure the stability of multidimensional dissipative solitons in the framework of the CGL equations [18–21], including vortex ("spinning") doughnut-shaped ones; see also reviews [22,23].

Check for updates

Received: 5 November 2026
Revised: 17 November 2026
Accepted: 19 November 2026
Published: 22 November 2026

Copyright: © 2026 by the authors. Licensee MDPI, Basel, Switzerland. This article is an open access article distributed under the terms and conditions of the Creative Commons Attribution (CC BY) license.

Another generic possibility to create stable 2D and 3D solitons is offered by models including spatially periodic (lattice) potentials, most frequently a periodic one. These potentials can represent laser cavities created in photonic crystals, induced by the spatially periodic modulation of the refractive index in the transverse direction [24,25], as well as a Bose–Einstein condensate (BEC) of excitons trapped in an optical lattice [26,27]. Solutions of the Gross–Pitaevskii equations with spatially and radially periodic potentials have been obtained in the form of stable vortex dissipative solitons [28]. In the spatiotemporal (effectively 3D) domain, relevant models include quasi-2D lattice potentials. Stable fundamental (zero-vorticity) and quasi-stable vortex solitons for such models are found in Refs. [29,30] and [31], respectively (see also the review [32]). A dissipative axisymmetric lattice, in the form of the radially periodic modulation of the gain and loss, rather than the reflective index, has been considered too [33,34]. In the latter case, the respective CGL equation produces localized star-shaped patterns with nonzero angular momentum but zero topological charge. Other low-dimensional potentials have also been considered, with razor, dagger and needle shapes [35], as well as azimuthally varying and conical ones [36].

The motion of solitons in the CGL model with a 2D transverse potential was considered in Ref. [37]. It was found that the fundamental soliton, hopping between potential cells, leaves arrayed patterns of different sizes in its wake. The motion of dipole and vortex dissipative solitons in the same model demonstrates a similar pattern formation scenario [38,39]. It is worth noting that Newton's cradle dynamics were observed in the train of secondary solitons generated by a moving primary one. A similar dynamical regime was predicted in soliton trains hosted by optical fibers [40].

Interactions between dissipative solitons determine the two- and multi-soliton dynamics. In the framework of the CGL models, bound states of dissipative solitons were predicted long ago [41,42] and observed in fiber lasers [43,44]; see also the recent review [45]. Other types of interaction, such as their merging and mutual destruction, have also been predicted [37,38] and observed in a passive optical cavity [46].

In the present work, we consider the motion of dissipative solitons in the 2D cubic–quintic CGL model with quasi-1D potentials. In Sections 2 and 3, we address, respectively, the dynamics of a single fundamental soliton and a soliton pair in a quasi-1D potential. The subject of Section 4 is the dynamics of a dissipative soliton in a potential in the form of a radial lattice. The paper is concluded in Section 5.

2. Motion of the Fundamental Soliton in the Quasi-1D Potential

We consider the cubic–quintic CGL equation, for amplitude $u(x,y;t)$ of the optical field, in its usual form,

$$\frac{\partial u}{\partial t} = -[\delta + iV(x,y)]u + (i+\varepsilon)|u|^2u - (i\nu+\mu)|u|^4u + \frac{i}{2}\Delta u, \tag{1}$$

where t is the propagation distance in optics, Δ is the Laplacian operator, and the quasi-1D lattice potential is

$$V(x,y) = -V_0\cos(2y), \tag{2}$$

whose period is fixed to π by rescaling. This period is commensurate with the numerical box size. The model applies, as a general one, to two-dimensional laser cavities [12,18–20,23,27,28,33,35–39]. In these numerous previously published works, physical conditions for the applicability of such models have been considered in detail; therefore, we refer the reader to these works for further information. Diffusion can be added to the model by replacing the imaginary coefficient in front of the Laplacian in Equation (1) with a complex one; see the review [47]. However, the diffusion of light does not occur in laser cavities and hence will not be accounted for here. The scaling is also used to fix the cubic

self-focusing and diffraction coefficients in Equation (1) to 1. Generic results are presented below, obtained by varying the depth V_0 of the lattice potential (2), for fixed characteristic values

$$\delta = 0.4, \varepsilon = 1.85, \nu = 0.1, \text{ and } \mu = 1 \tag{3}$$

of the linear loss, cubic gain, quintic defocusing and quintic loss coefficients, respectively.

Simulations of Equation (1) were performed by means of the standard fourth-order Runge-Kutta algorithm with an adaptive step for variable t, while the second derivatives with respect to x and y were computed using five-point finite-differences formulas, with periodic boundary conditions. We use a 292×292 numerical grid centered at (0,0) with a box size given by $\max(x) = \max(y) = 21.991 = 7\pi$ for the periodic potential. For the circular potential, the grid is 280×280 and the box size $\max(x) = \max(y) = 20.955$, with the center still being (0,0). In this case, a few computations are performed with a smaller grid of 140×140, with $\max(x) = \max(y) = 10.477$. An example of the stable fundamental soliton produced by the numerical scheme for $V_0 = 1$ is displayed in Figure 1. To set the dissipative soliton in motion, we apply the kick to it,

$$u(x,y) \to u(x,y) \exp(i\mathbf{k}_0 \cdot \mathbf{r}), \ \mathbf{k}_0 = k_0(\cos\theta, \sin\theta), \ \mathbf{r} = (x,y), \tag{4}$$

and use expression (4) as the input for simulations of Equation (1). Systematic results are produced by varying the kick's strength k_0 and direction θ.

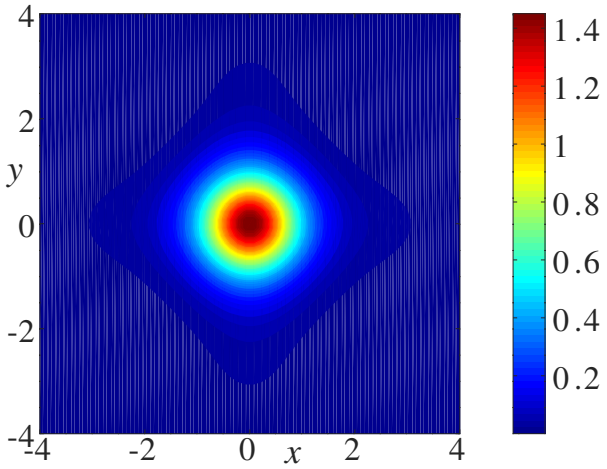


Figure 1. The stable fundamental dissipative 2D soliton produced by the numerical solution of Equation (1) with $V_0 = 1$ in the quasi-1D potential (2) and coefficients (3). Plotted is $|u|$, representing the solution as $u(x,y,t) = |u(x,y)| \exp(-i\omega t)$ with $\omega = -0.377$.

Figure 2 demonstrates that a sufficiently deep potential (2) (in particular, with $V_0 = 1$) keeps the dissipative soliton kicked across the potential ($\theta = \pi/2$ in Equation (4)). In this case, the kick initiates gradually decaying oscillations of the soliton in the vertical direction. This outcome occurs for $\theta = \pi/2$, $V_0 = 1$ and $0.1 \leqslant k_0 \leqslant 1.81$. The upper bound of this outcome is $k_0 = 1.53$ for the potential with an intermediate strength, $V_0 = 2/3$, and $k_0 = 0.6$ for $V_0 = 0.2$. Naturally, the period T of the damped oscillations increases for a weaker potential; for instance, a kick with $k_0 = 0.5$ gives rise to oscillations with $T = 8$, 12 and 25 for $V_0 = 1$, 0.66 and 0.2, respectively. These oscillations closely resemble the trapped waves reported for solitons interacting with an external force field in KdV-type models with localized [48] and periodic [49] potentials, except that, in these studies, the oscillation amplitude grows in time, while, in the present one, it is damped.

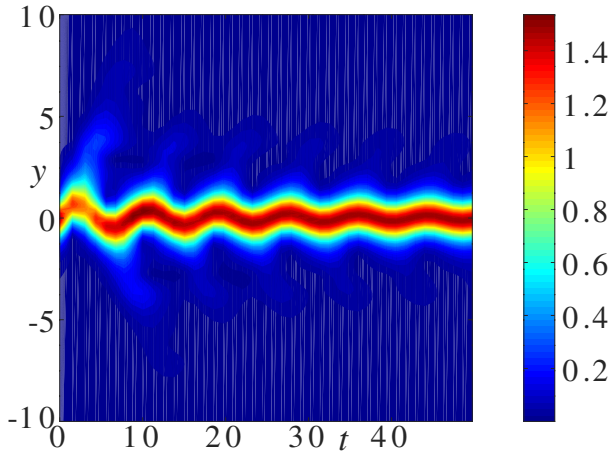


Figure 2. Transient oscillations of the soliton in the deep potential (2), with $V_0 = 1$, initiated by a relatively strong transverse kick (4) with $k_0 = 1.3$ and $\theta = \pi/2$. It eventually stops. Plotted is $|u(t, y)|$ in cross-section $x = 0$.

For the same, relatively deep quasi-1D potential as in Figure 2, with $V_0 = 1$, a stronger transverse kick (4), with $\theta = \pi/2$ and $1.82 \leqslant k_0 \leqslant 2.407$, applied to the initial soliton, overcomes the potential barrier by creating an additional soliton-like spot in the adjacent trough, in the direction of the kick. However, as shown in Figure 3, the thus-produced double soliton is unstable, disappearing after passing a small propagation distance t. For a more shallow quasi-1D potential, with $V_0 = 0.66$ in Equation (2), the application of the kick produces essentially the same outcome in the interval $1.54 \leq k_0 \leq 1.81$.

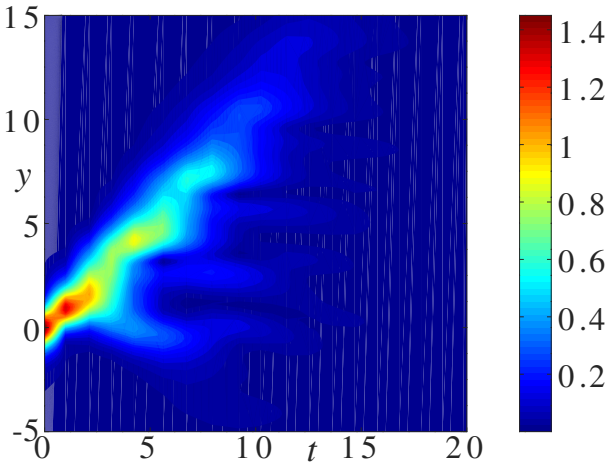


Figure 3. The creation of an additional soliton in an adjacent potential trough by the application of a strong kick (4), with $k_0 = 2.2$ and $\theta = \pi/2$, to the potential (2) with $V_0 = 1$, followed by the quick decay of the entire pattern. Plotted is $|u(t, y)|$ in cross-section $x = 0$.

Finally, Figure 4 demonstrates that the strongest kicks considered in this work, in the interval of $2.408 \leq k_0 \leq 3$, if again applied to the dissipative soliton under the the action of the quasi-1D potential (2), lead to another output: after a transient stage of attenuation and revival, the initial soliton is converted into a quasi-steadily moving one. Naturally, its velocity increases with the kick's magnitude k_0, while the duration of the transient stage reduces. For a weaker potential, the steady-propagation regime commences from smaller values of k_0—e.g., it occurs at $k_0 \geq 1.82$ for $V_0 = 0.66$.

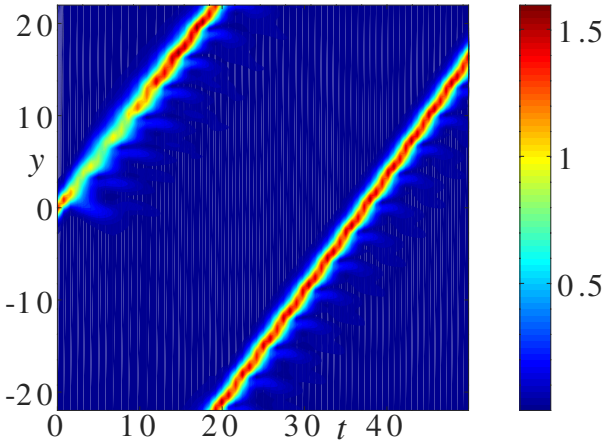


Figure 4. The strong transverse kick (4), with $k_0 = 2.5$ and $\theta = \pi/2$, applied to the relatively deep quasi-1D potential (2), with $V_0 = 1$, sets the dissipative soliton in the state of quasi-steady motion. Plotted is $|u(t, y)|$ in cross-section $x = 0$.

The 2D CGL model based on Equation (1) with a shallow quasi-1D potential (2) (e.g., with $V_0 = 0.2$) produces different phenomenology for kicked dissipative solitons. The destruction regime, illustrated in Figure 3, does not occur in this case. Instead, the kick sets the soliton in a state of low motion, without causing its decay. For instance, the transverse ($\theta = \pi/2$) kick with $k_0 = 0.70$ and 0.78 imparts small velocities to the soliton, with which it passes, respectively, a single cell or three cells of the lattice within the full simulation, up to $t = 50$. In the same case of $V_0 = 0.2$, stronger kicks, in the interval of $0.79 \leqslant k_0 \leqslant 0.94$, lead to the duplication of the soliton, being somewhat similar to the initial stage observed in Figure 3 (for $V_0 = 1$), but it is not followed by the disappearance of the soliton. For $k_0 \leqslant 0.84$, two solitons persist. Counterintuitively, the observed motion is faster for $k_0 = 0.79$ than for larger magnitudes of the kick. From $k_0 = 0.85$ up to $k_0 = 0.89$, the rear spot is eventually reabsorbed by the front one, while, at $k_0 > 0.89$, both solitons persist, with the front one moving steadily and the rear one demonstrating slow oscillations; see Figure 5. Note that soliton splitting has also been reported for the average field of Benjamin–Ono solitons affected by random perturbations [50]. Eventually, at $k_0 \geqslant 0.95$, the rear soliton vanishes so that the simulations produce a single moving soliton.

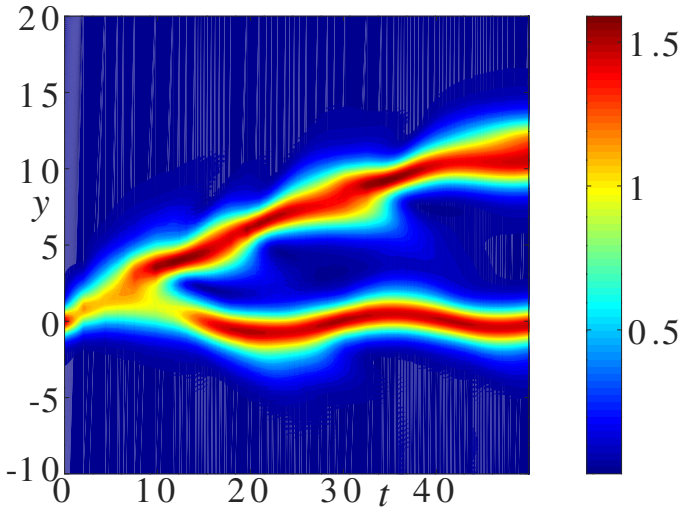


Figure 5. The duplication of a stable dissipative soliton by kick (4) with $k_0 = 0.94$ and $\theta = \pi/2$, applied to the shallow potential with $V_0 = 0.2$ in Equation (2). Plotted is $|u(t, y)|$ in cross-section $x = 0$.

The above results are produced for the transverse kick with $\theta = \pi/2$ in Equation (4). The longitudinal kick, with $\theta = 0$, immediately sets the soliton in free motion, as Equation (1) keeps Galilean invariance in the x direction—cf. Ref. [18]. An oblique kick (e.g., with $\theta = \pi/4$) leads to the straightforward superposition of the motions in the y and x directions.

Figure 6 shows the different outcomes of kicking the single 2D soliton in the transverse direction ($\theta = \pi/2$), in the plane of two parameters V_0 and k_0, while the other parameters are fixed as per Equation (3).

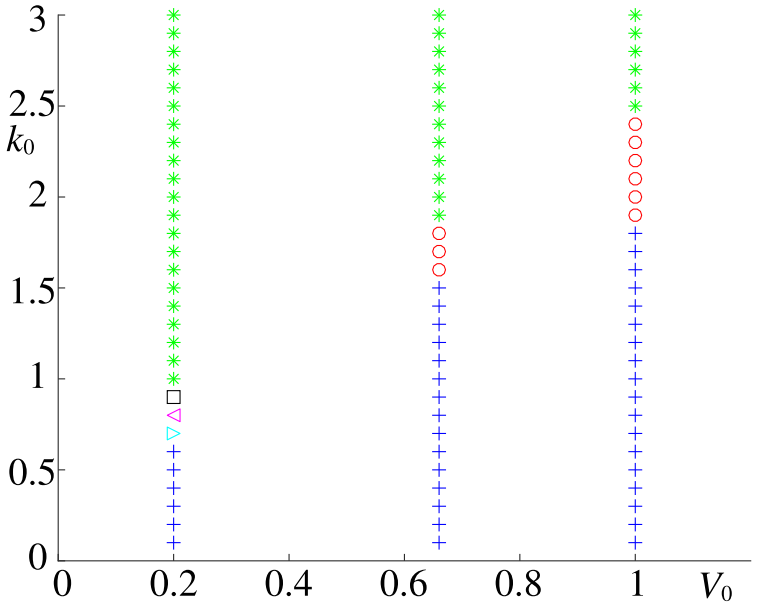


Figure 6. The different outcomes of kicking a single 2D soliton in the transverse direction ($\theta = \pi/2$), versus V_0 and k_0. +: damped oscillations; ∘: disappearance of the soliton; ∗: soliton motion; ▷: slow motion; ◁: two-soliton final state; □: duplication and slow motion of the front soliton.

3. The Quasi-1D Potential: Dynamics of Soliton Pairs

To study the two-soliton dynamics, we prepare an input containing two solitons in adjacent troughs of the quasi-1D potential (2), with identical phases. Then, the soliton pair is set in motion by the application of kick (4) to both solitons. The longitudinal kick with $\theta = 0$ (at least in the interval of $0.1 \leq k_0 \leq 5$) creates a pair of synchronously moving solitons, irrespective of whether the solitons form a true bound state or not.

Of particular interest are the effects produced by the transverse kick, with $\theta = \pi/2$. If the kick is weak, $0.1 \leqslant k_0 \leqslant 1.4$, the widths and vertical positions of the two solitons oscillate, but the solitons do not pass the potential barrier.

In the interval of $1.5 \leqslant k_0 \leqslant 1.8$, the stronger kick initiates complex dynamics, including soliton multiplication. At $k_0 = 1.5$, the kicked solitons first move forward, leaving copies of themselves in place, thus yielding a train of four spots. Then, they move backward, in the form of a pair of quasi-solitons, as shown in Figure 7. While backward propagation also occurs at $k_0 = 1.51$, in the interval of $1.52 \leq k_0 \leq 1.55$, the initial soliton pair propagates forward, generating a quiescent soliton train in its wake, as seen in Figure 8.

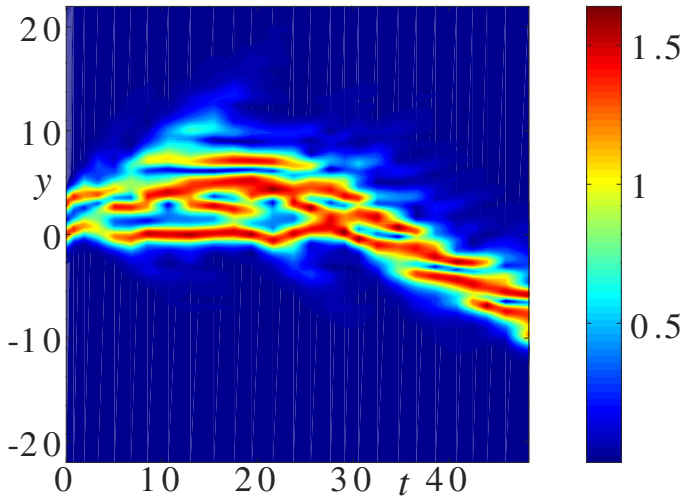


Figure 7. The kicked soliton pair, with $V_0 = 1$, $k_0 = 1.5$ and $\theta = \pi/2$, creates another pair, moving forward, and then inverts the direction of motion, while the additional pair disappears. Plotted is $|u(t, y)|$ in cross-section $x = 0$.

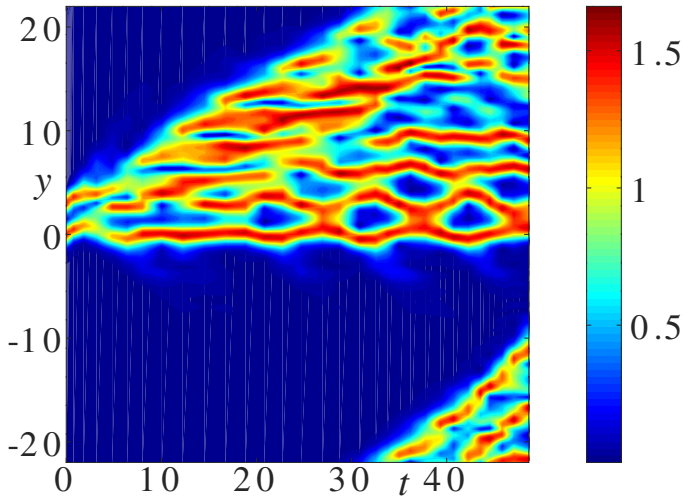


Figure 8. The forward motion of the soliton pair generates a train of quiescent solitons, as shown here for $k_0 = 1.54$, $\theta = \pi/2$ and $V_0 = 1$. Plotted is $|u(t, y)|$ in cross-section $x = 0$.

At $k_0 \geq 1.56$, empty sites appear between the moving soliton and the train. The train length increases with k_0, reaching a maximum value corresponding to 10 solitons in the interval of $1.71 \leq k_0 \leq 1.73$. Then, the length decreases, while the number of moving solitons is reduced to one. Eventually, the train is reduced to a single soliton at $1.9 \leq k_0 \leq 2.5$. At still larger values of k_0, the fixed soliton disappears and we are left with a single moving soliton. This behavior has been checked up to $k_0 = 3.5$.

As well as in the case of the single-soliton dynamics, the result of the application of the oblique kick (4), with $\theta \neq \pi/2$, can be understood as the superposition of the dynamics in the transverse (y) direction and free motion along x. A new possibility, displayed in Figure 9, is the collision between solitons moving in different directions as a result of the application of an oblique ($\theta = \pi/4$), relatively strong kick (4), $2.6 \leqslant k_0 \leqslant 3.5$: one soliton moves along the x-axis and the other in the diagonal direction. The background potential (2) is relatively strong too, with $V_0 = 1$. It is seen that the collision is quasi-elastic, although a conspicuous excitation is generated in the soliton moving in the diagonal direction.

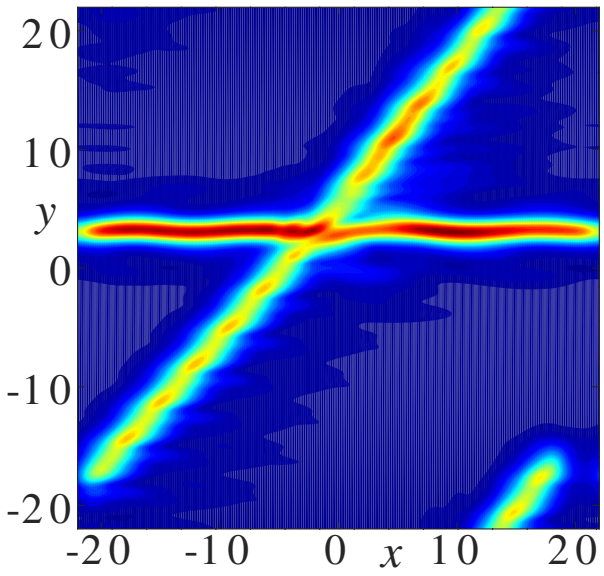


Figure 9. An example of a quasi-elastic collision between solitons initially moving along the diagonal, $y = x$, and one moving along the x-axis. Plotted is $\int_{27.2}^{43.6} |u(x, y; t)|dt$, allowing the visualization of the trajectories in the (x, y) plane. The kick (4) with $k_0 = 3.5$ and $\theta = \pi/4$ was initially applied to the moving solitons. The depth of the underlying quasi-1D potential is $V_0 = 1$. The trajectory of the moving solitons reappears due to periodic boundary conditions.

4. The Circular Potential

In this section, we consider the 2D CGL Equation (1) with the potential representing a radial lattice,

$$V = V_0 \cos^2\left(\frac{r}{2}\right), \; r = \sqrt{x^2 + y^2}. \tag{5}$$

We use the same parameter values (3) as fixed above and set $V_0 = 1$. The potential has minima at circumferences $r = \pi(1 + 2n)$. The periodic boundary conditions strongly perturb the propagation when the soliton moves too far from the center of the potential. The results of the computations are disregarded as soon as this occurs.

First, we consider a fundamental (zero-vorticity) dissipative soliton trapped in the first circular potential trough, with the minimum at $r = \pi$. The soliton is set in motion along the trough by applying kick (4) to it in the tangential direction, with $\theta = \pi/2$. In the interval of the kick's strength $0.1 \leqslant k_0 \leqslant 1.5$, the soliton performs steady circular motion (resembling the "rotary solitons" known in conservative models [51]), as shown in Figure 10.

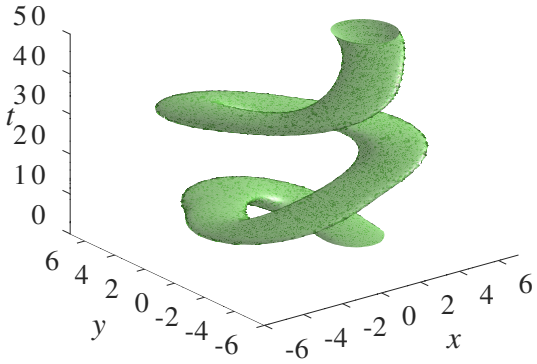


Figure 10. The circular motion of the fundamental dissipative soliton initiated by the kick (4), with $k_0 = 1.3$ and $\theta = \pi/2$. Plotted is the equidensity surface $|u(x, y; t)| = 0.5$, which is produced by the numerical solution of Equation (1) with coefficients (3) and potential (5) with $V_0 = 1$.

Its speed increases with k_0 but eventually saturates for the largest values of k_0. At $k_0 = 1.5$, the moving soliton emits a fleeting spot in the neighbor channel. For larger k_0 (e.g., $k_0 = 1.6$), Figure 11 demonstrates that the soliton, under the action of centrifugal force, moves across the radial lattice potential.

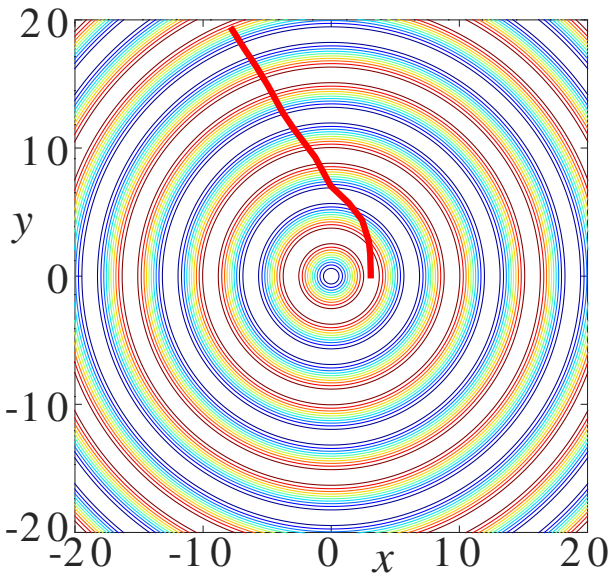


Figure 11. The motion of the soliton across the radial lattice, due to the action of a large centrifugal force, corresponding to the kick magnitude $k_0 = 1.6$. Plotted (red line) is the trajectory of the soliton's maximum in the (x, y) plane. Circles represent the potential.

From $k_0 = 1.7$ to 2.3, the trajectory is still deviated by the potential, but the deviation reduces as k_0 increases. From $k_0 = 2.4$ to 3, the trajectory, driven by the strong centrifugal force, remains almost rectilinear up to the end of the simulation. The simulation was terminated when the spot hit the boundary, as shown in Figure 12.

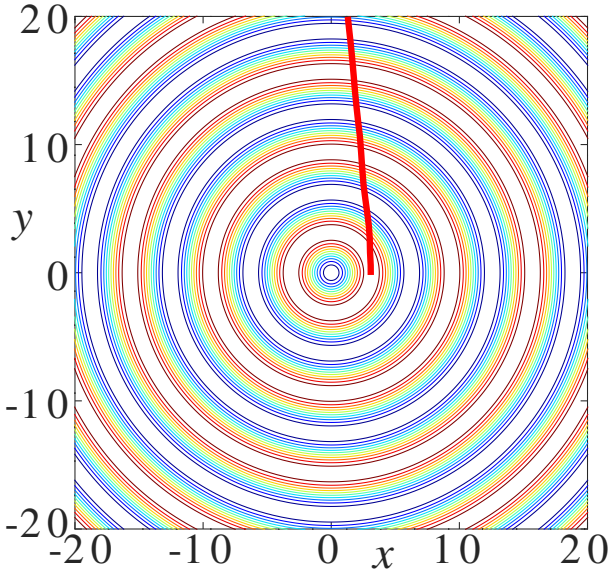


Figure 12. The soliton's trajectory is nearly straight in the case of a very strong kick, $k_0 = 2.8$. Plotted (red line) is the trajectory of the soliton maximum in the (x, y) plane. Circles represent the potential.

Next, we consider the action of a kick directed towards the center of the potential (with $\theta = \pi$). For $0.1 \leqslant k_0 \leqslant 1.1$, we observe damped oscillations in the radial direction (transversely to the circular potential trough); see Figure 13. Deformations of the soliton are visible too, especially for larger values of k_0.

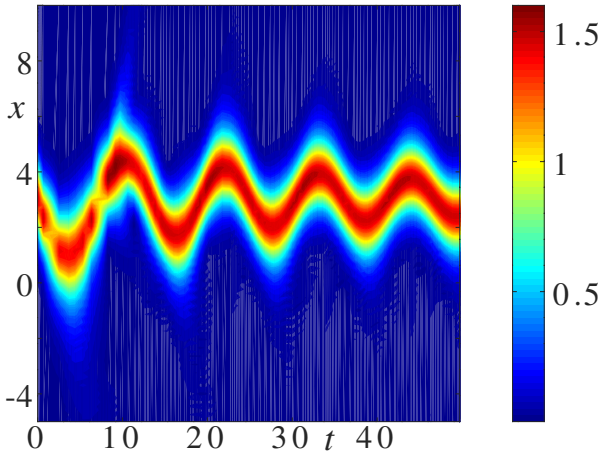


Figure 13. The soliton oscillates in the transverse (radial) direction initiated by the application of a kick with $k_0 = 1.1$ towards $r = 0$ (across the circular potential). Plotted is $|u(x,t)|$ in cross-section $y = 0$.

A stronger inward kick, with $k_0 = 1.2$, sends the dissipative soliton towards the center. It bounces back from the central potential hill, warps into a crescent and then splits into two solitons. One of them initiates circular motion around the potential trough, while the other one disappears straight away; see Figure 14. The choice of a particular direction of the circular motion implies the occurrence of spontaneous symmetry breaking.

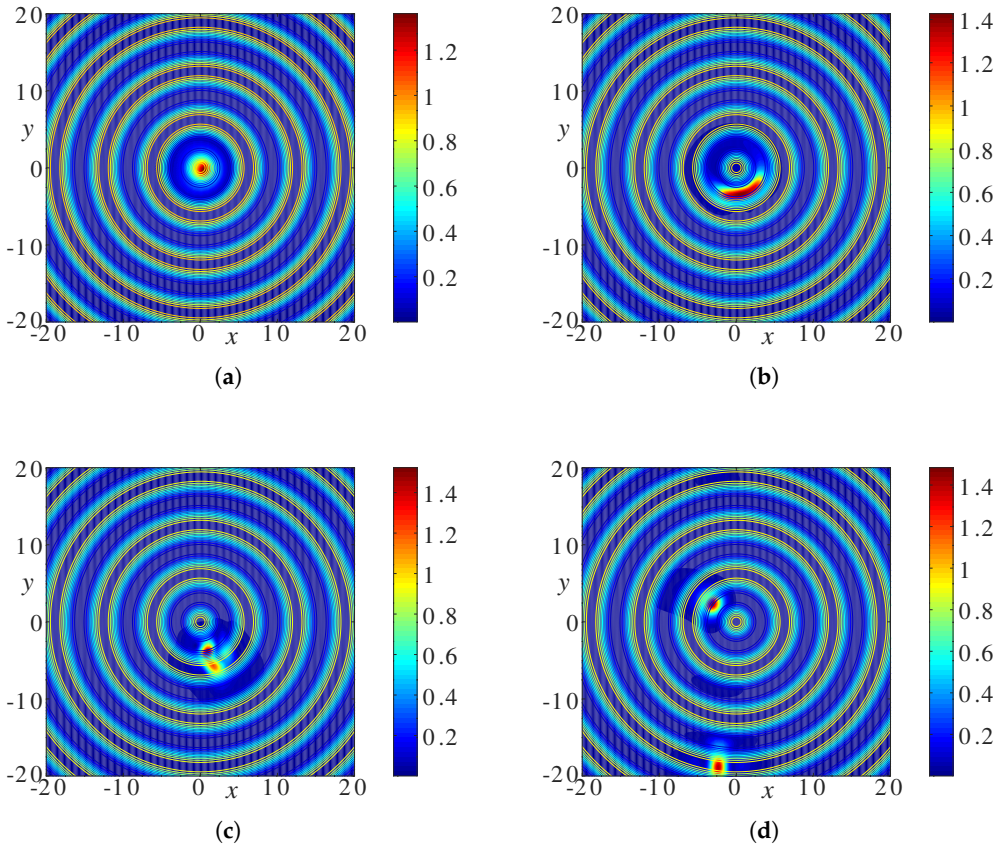


Figure 14. The soliton kicked towards the center by the push (4) with $k_0 = 1.2$ and $\theta = \pi$ bounces off the central potential hill [(**a**), $t = 3.65$], takes a crescent shape [(**b**), $t = 8.66$] and duplicates [(**c**), $t = 12.45$]; then, one soliton moves around the potential trough while the other disappears straight away [(**d**), $t = 23.53$]. Plotted is $|u(x,y)|$ in the (x,y) plane.

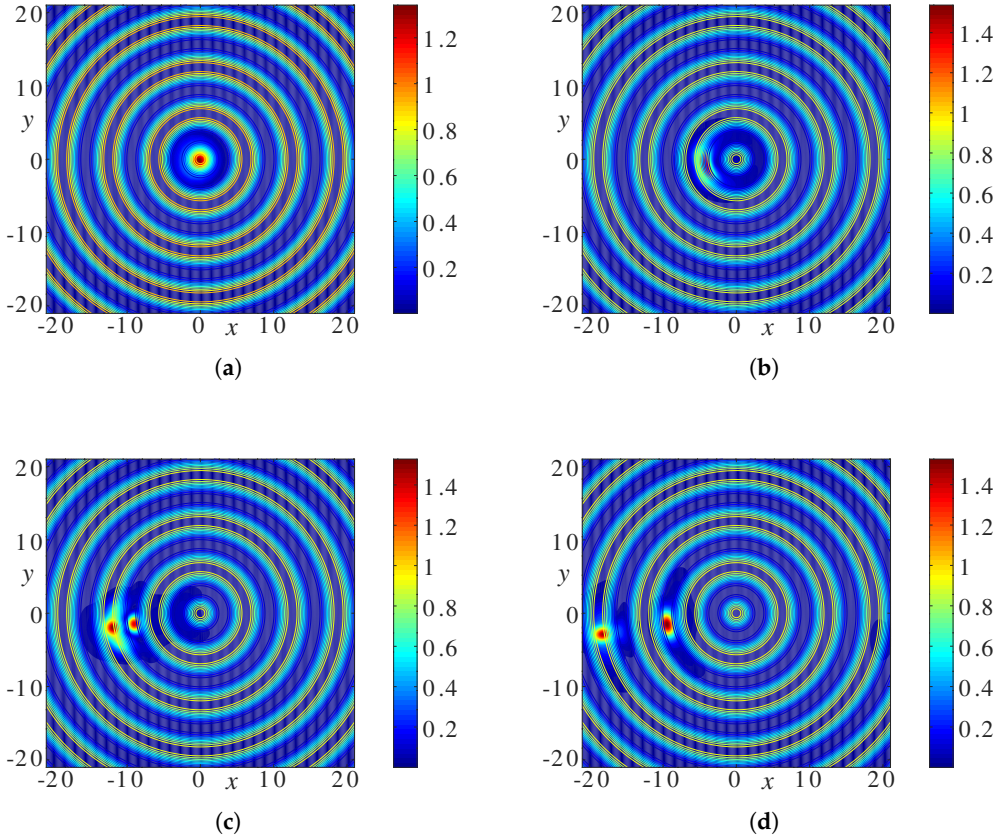


Figure 15. The soliton kicked inward as per Equation (4), with $k_0 = 1.5$ and $\theta = \pi$, passes the central potential hill [see panel (**a**), corresponding to $t = 2.88$] and stops at the first annular potential barrier, spreading into a crescent-shaped structure [(**b**), $t = 6.12$]. Then, the crescent splits into two fragments [(**c**), $t = 15.52$], one of which stays motionless in the annular potential trough, while the second one moves straight [(**d**), $t = 20.77$], in a direction that is oblique with respect to the x-axis, featuring symmetry breaking. Plotted is $|u(x, y; t)|$ in the (x, y) plane.

The evolution initiated by the strong inward kick with $k_0 \geq 1.5$ is represented in Figure 15. In this case, the kicked soliton acquires sufficient momentum to pass the central potential hill, gradually losing momentum in the course of motion. It continues straight until the momentum is insufficient to pass a particular circular barrier, where it stops, spreading into a crescent. Naturally, the distance passed before the stoppage increases with k_0. In the case of $k_0 = 1.5$, Figure 15 demonstrates that, after the kicked soliton passes the central hill, it stops at the first annular potential barrier and spreads into a crescent, which splits into two spots. One of them remains motionless in the annular channel, and the other one keeps moving straight. Its direction is not parallel to the x-axis, featuring symmetry breaking. For a higher inward kick, the initial spot continues propagating in the left direction up to the boundary of the numerical box.

5. Discussion

In the quasi-1D lattice potential, the 2D dissipative soliton set in motion by the transverse kick (4), with $\theta = \pi/2$, stays in the original potential trough if the kick's strength k_0 is small. In contrast, the soliton kicked with a large k_0 moves freely across the potential lattice. At intermediate values of k_0, more complex dynamics occur, with jumps between adjacent troughs and soliton duplication. Regarding the soliton pair, only a single freely moving soliton can be produced by the kick, and the dynamics of the intermediate regime are more complex, involving the formation of a soliton train.

When the kick is applied parallel to the quasi-1D potential ($\theta = 0$ in Equation (4)), both the single soliton and the soliton pair move freely along the direction that admits Galilean invariance. An oblique kick ($0 < \theta < \pi/2$) typically initiates motion that consists of the straightforward superposition of the two transverse and longitudinal modes. A separately considered case is the collision between two dissipative solitons moving in the diagonal and longitudinal directions.

In the radial lattice potential, the application of a relatively weak kick in the tangential directions initiates motion along an annular potential trough. However, a stronger tangential kick produces fast motion with a large centrifugal force, which drives the solitons along complex trajectories crossing the radial potential barrier.

When the strong kick is directed towards the center of the radial lattice, it pushes the dissipative soliton across the central potential hill. Eventually, the soliton stops at a certain annular potential barrier, spreading into a crescent structure, which, in turn, may split into two fragments, one of which remains motionless while the second one keeps moving in a slightly oblique direction. The outcome of the evolution features spontaneous symmetry breaking.

As an extension of this analysis, it may be interesting to explore the evolution of 2D dissipative solitons carrying embedded vorticity. In particular, the longitudinal motion along the free direction of the quasi-1D potential may be perturbed in the transverse direction by an effective "Magnus force".

Supplementary Materials: The following supporting information can be downloaded at: https://www.mdpi.com/article/10.3390/photonics13121097/s1.

Author Contributions: Conceptualization, B.A.M. and V.B.; software, V.B.; investigation, V.B. and H.L.; writing, H.L., B.A.M. and D.M. All authors have read and edited the published version of the manuscript.

Funding: This research received no external funding.

Data Availability Statement: The original contributions presented in this study are included in the article/supplementary material. Further inquiries can be directed to the corresponding author(s).

Conflicts of Interest: The authors declare no conflicts of interest.

References

1. Aranson, I.S.; Kramer, L. The world of the complex Ginzburg-Landau equation. *Rev. Mod. Phys.* **2002**, *74*, 99–143.
2. Malomed, B.A. Evolution of nonsoliton and "quasiclassical" wavetrains in nonlinear Schrödinger and Korteweg—De Vries equations with dissipative perturbations. *Phys. D* **1987**, *29*, 155–172.
3. Thual, O.; Fauve, S. Localized structures generated by subcritical instabilities. *J. De Phys.* **1988**, *49*, 1829–1833.
4. Akhmediev, N.; Afanasjev, V.V.; Soto-Crespo, J.M. Singularities and special soliton solutions of the cubic-quintic complex Ginzburg-Landau equation. *Phys. Rev. E* **1996**, *53*, 1190–1201.
5. Soto-Crespo, J.M.; Akhmediev, N.; Afanasjev, V.V.; Wabnitz, S. Pulse solutions of the cubic-quintic complex Ginzburg-Landau equation in the case of normal dispersion. *Phys. Rev. E* **1997**, *55*, 4783–4796.
6. Akhmediev, N.N.; Ankiewicz, A. *Solitons: Nonlinear Pulses and Beams*; Chapman & Hall: London, UK, 1997.
7. Descalzi, O.; Argentina, M.; Tirapegui, E. Stationary localized solutions in the subcritical complex Ginzburg-Landau equation. *Int. J. Bifurc. Chaos* **2002**, *12*, 2459–2465.
8. Silberberg, Y. Collapse of optical pulses. *Opt. Lett.* **1990**, *15*, 1282–1284.
9. Stegeman, G.I.; Christodoulides, D.N.; Segev, M. Optical Spatial Solitons: Historical Perspectives. *IEEE J. Select. Top. Quant. Electron.* **2000**, *6*, 1419.
10. Fibich, G. *The Nonlinear Schrödinger Equation: Singular Solutions and Optical Collapse*; Springer: Berlin/Heidelberg, Germany, 2015.
11. Buryak, A.V.; Kivshar, Y.S.; Trillo, S. Optical solitons supported by competing nonlinearities. *Opt. Lett.* **1995**, *20*, 1961.
12. Skarka, V.; Berezhiani, V.I.; Miklaszewski, R. Spatiotemporal soliton propagation in saturating nonlinear optical media. *Phys. Rev. E* **1997**, *56*, 1080.

13. Quiroga-Teixeiro, M.; Michinel, H. Stable azimuthal stationary state in quintic nonlinear optical media. *J. Opt. Soc. Am. B* **1997**, *14*, 2004–2009.
14. Quiroga-Teixeiro, M.L.; Berntson, A.; Michinel, H. Internal dynamics of nonlinear beams in their ground states: Short- and long-lived excitation. *J. Opt. Soc. Am. B* **1999**, *16*, 1697–1703.
15. Montesinos, G.D.; Pérez-García, V.M.; Michinel, H. Stabilized two-dimensional vector solitons. *Phys. Rev. Lett.* **2004**, *92*, 133901.
16. Mihalache, D.; Mazilu, D.; Crasovan, L.-C.; Towers, I.; Buryak, A.V.; Malomed, B.A.; Torner, L.; Torres, J.P.; Lederer, F. Stable spinning optical solitons in three dimensions. *Phys. Rev. Lett.* **2002**, *88*, 073902.
17. Falc ao-Filho, E.L.; de Araújo, C.B.; Boudebs, G.; Leblond, H.; Skarka, V. Robust two-dimensional spatial solitons in liquid carbon disulfide. *Phys. Rev. Lett.* **2013**, *110*, 013901.
18. Sakaguchi, H. Motion of pulses and vortices in the cubic-quintic complex Ginzburg-Landau equation without viscosity. *Phys. D* **2005**, *210*, 138–148.
19. Grelu, P.; Soto-Crespo, J.M.; Akhmediev, N. Light bullets and dynamic pattern formation in nonlinear dissipative systems. *Opt. Express* **2005**, *13*, 9352.
20. Soto-Crespo, J.M.; Grelu, P.; Akhmediev, N. Optical bullets and "rockets" in nonlinear dissipative systems and their transformations and interactions. *Opt. Express* **2006**, *14*, 4013.
21. Mihalache, D.; Mazilu, D.; Lederer, F.; Kartashov, Y.V.; Crasovan, L.-C.; Torner, L.; Malomed, B.A. Stable vortex tori in the three-dimensional cubic-quintic Ginzburg-Landau equation. *Phys. Rev. Lett.* **2006**, *97*, 073904.
22. Mihalache, D. Three-dimensional dissipative optical solitons. *Cent. Eur. J. Phys.* **2008**, *6*, 582–587.
23. Malomed, B.A. Multidimensional dissipative solitons and solitary vortices. *Chaos, Solitons Fractals* **2022**, *163*, 112526.
24. Wise, F.W.; Chong, A.; Renninger, W.H. High-energy femtosecond fiber lasers based on pulse propagation at normal dispersion. *Laser Phot. Rev.* **2008**, *2*, 58–73,
25. Forbes, A.; Mkhumbuza, L.; Feng, L. Orbital angular momentum lasers. *Nat. Rev. Phys.* **2024**, *6*, 352–364.
26. Dalfovo, F.; Giorgini, S.; Pitaevskii, L.P.; Stringari, S. Theory of Bose-Einstein condensation in trapped gases. *Rev. Modern Phys.* **1999**, *71*, 463.
27. Carusotto, I.; Ciuti, C. Quantum fluids of light. *Rev. Mod. Phys.* **2013**, *85*, 299.
28. Mihalache, D.; Mazilu, D.; Skarka, V.; Malomed, B.A.; Leblond, H.; Aleksić, N.B.; Lederer, F. Stable topological modes in two-dimensional Ginzburg-Landau models with trapping potentials. *Phys. Rev. A* **2010**, *82*, 023813.
29. Baizakov, B.B.; Malomed, B.A.; Salerno, M. Multidimensional solitons in a low-dimensional periodic potential. *Phys. Rev. A* **2004**, *70*, 053613.
30. Mihalache, D.; Mazilu, D.; Lederer, F.; Kartashov, Y.V.; Crasovan, L.-C.; Torner, L. Stable three-dimensional spatiotemporal solitons in a two-dimensional photonic lattice. *Phys. Rev. E* **2004**, *70*, 055603(R).
31. Leblond, H.; Malomed, B.A.; Mihalache, D. Three-dimensional vortex solitons in quasi-two-dimensional lattices. *Phys. Rev. E* **2007**, *76*, 026604.
32. Mihalache, D. Three-dimensional Ginzburg-Landau dissipative solitons supported by a two-dimensional transverse grating. *Proc. Rom. Acad. A* **2010**, *11*, 142–147.
33. Skarka, V.; Aleksić, N.B.; Lekić, M.; Aleksić, B.N.; Malomed, B.A.; Mihalache, D.; Leblond, H. Formation of complex two-dimensional dissipative solitons via spontaneous symmetry breaking. *Phys. Rev. A* **2014**, *90*, 023845.
34. Skarka, V.; Aleksić, N.B.; Leblond, H.; Malomed, B.A.; Mihalache, D. Varieties of stable vortical solitons in Ginzburg-Landau media with radially inhomogeneous losses. *Phys. Rev. Lett.* **2010**, *105*, 213901.
35. Liu, B.; He, Y.J.; Malomed, B.A.; Wang, X.S.; Kevrekidis, P.G.; Wang, T.B.; Leng, F.C.; Qiu, Z.R.; Wang, H.Z. Continuous generation of soliton patterns in two-dimensional dissipative media by razor, dagger, and needle potentials. *Opt. Lett.* **2010**, *35*, 1974–1976.
36. Liu, B.; He, X.D. Continuous generation of "light bullets" in dissipative media by an annularly periodic potential. *Opt. Express* **2011**, *19*, 20009–20014.
37. Besse, V.; Leblond, H.; Mihalache, D.; Malomed, B.A. Pattern formation by kicked solitons in the two-dimensional Ginzburg-Landau medium with a transverse grating. *Phys. Rev. E* **2013**, *87*, 012916.
38. Besse, V.; Leblond, H.; Mihalache, D.; Malomed, B.A. Building patterns by traveling dipoles and vortices in two-dimensional periodic dissipative media. *Opt. Comm.* **2014**, *332*, 279–291.
39. Mihalache, D. Localized optical structures: An overview of recent theoretical and experimental developments. *Proc. Rom. Acad. A* **2015**, *16*, 62–69.
40. Driben, R.; Malomed, B.A.; Yulin, A.V.; Skryabin, D.V. Newton's cradles in optics: From to N -soliton fission to soliton trains. *Phys. Rev. A* **2013**, *87*, 063808.
41. Afanasjev, V.V.; Malomed, B.A.; Chu, P.L. Stability of bound states of pulses in the Ginzburg-Landau equations. *Phys. Rev. E* **1997**, *56*, 6020–6025.
42. Akhmediev, N.; Ankiewicz, A.; Soto-Crespo, J. Multisoliton solutions of the complex Ginzburg-Landau equation. *Phys. Rev. Lett.* **1997**, *79* 4047–4051.

43. Gong, Y.; Shum, P.; Hiang, T.; Cheng; Wen, Q.; Tang, D.Y. Bound soliton pulses in passively mode-locked fiber laser. *Opt. Commun.* **2001**, *200*, 389–400.
44. Hideur, A.; Ortaç, B.; Chartier, T.; Brunel, M.; Leblond, H.; Sanchez, F. Ultra-short bound states generation with a passively mode-locked high-power Yb-doped double-clad fiber laser. *Opt. Commun.* **2003**, *225*, 71–78.
45. Cui, Y.; Lu, T.; Zhang, Y.; Mao, D.; Malomed, B.A. Bound states of solitons in fiber lasers. *Phys. Rep.* **2026**, *1184*, 1–58.
46. Jang, J.K.; Erkintalo, M.; Luo, K.; Oppo, G.-L.; Coen, S.; Murdoch, S. Controlled merging and annihilation of localised dissipative structures in an AC-driven damped nonlinear Schrödinger system. *New J. Phys.* **2016**, *18*, 033034.
47. Rosanov, N.N.; Fedorov, S.V.; Veretenov, N.A. Dissipative optical solitons: From scalar 1D- to 2D- and 3D-, topological and vector solitons. *Phys. Rep.* **2026**, *1162*, 1–60.
48. Flamarion, M.V.; Pelinovsky, E. Interactions of solitons with an external force field: Exploring the Schamel equation framework. *Chaos, Solitons Fractals* **2023**, *174*, 113799 .
49. Flamarion, M.V.; Pelinovsky, E. Solitary wave interactions with an external periodic force: The extended Korteweg-de Vries framework. *Mathematics* **2022**, *10*, 4538.
50. Flamarion, M.V.; Pelinovsky, E.; Didenkulova, E. Soliton dynamics in random fields: The Benjamin-Ono equation framework. *Appl. Math. Model.* **2025**, *144*, 116092.
51. Kartashov, Y.V.; Vysloukh, V.A.; Torner, L. Rotary solitons in Bessel optical lattices. *Phys. Rev. Lett.* **2004**, *93*, 093904.

Disclaimer/Publisher's Note: The statements, opinions and data contained in all publications are solely those of the individual author(s) and contributor(s) and not of MDPI and/or the editor(s). MDPI and/or the editor(s) disclaim responsibility for any injury to people or property resulting from any ideas, methods, instructions or products referred to in the content.